

Enhanced Harmonic Generation from $M = 1$ aligned Ar^+

A. C. Brown and H. W. van der Hart

*Centre for Theoretical Atomic, Molecular and Optical Physics,
Queen's University Belfast, Belfast, BT7 1NN, UK.*

(Dated:)

We investigate harmonic generation (HG) from ground-state Ar^+ aligned with $M = 1$ at a laser wavelength of 390-nm and intensity of $4 \times 10^{14} \text{ Wcm}^{-2}$. Using time-dependent R-matrix theory, we find that an initial state with magnetic quantum number $M = 1$ provides a 4-fold increase in harmonic yield over $M = 0$. HG arises primarily from channels associated with the $^3P^e$ threshold of Ar^{2+} , in contrast with $M = 0$ for which channels associated with the excited, $^1D^e$ threshold dominate HG. Multichannel and multielectron interferences lead to a more marked suppression of HG for $M = 1$ than $M = 0$.

PACS numbers: 32.80.Rm, 31.15.A-, 42.65.Ky

I. INTRODUCTION

Recent advances in laser technology have facilitated the experimental analysis of atomic structure and electron dynamics in more detail than ever before [1]. The process of harmonic generation (HG) has been central to these advances both as a basis for ultrashort and high energy light pulses [2, 3], and as a tool for elucidating ultrafast dynamics [4–6]. These dynamics can be strongly influenced by the interaction of channels associated with different ionization thresholds [7–10]. Hence, the development of methods capable of investigating the influence of channel coupling on HG is of strong current interest.

Traditionally, the HG process is thought of as a single electron process [11], and a variety of theoretical methods for addressing the process have been based on this approach [12–14]. The ‘three-step’, or recollision, model of HG outlined in [11] describes a laser-ejected electron being driven by the field before recolliding with its parent ion. Upon recollision the electron can be recaptured, emitting its energy in the form of an odd harmonic of the driving laser frequency. Despite the success of this approach, recent research has uncovered more complex multielectron and multichannel influences in HG [7, 8, 10]. Thus there is a need for quality theoretical data to direct experimental attosecond science, and to enhance our understanding of these fundamental physical processes.

It is for these reasons that we have developed time-dependent R-matrix (TDRM) theory [15]– a fully non-perturbative, *ab initio* method for the description of general multielectron atoms in short, intense laser pulses. TDRM has been used successfully to elucidate the collective electron-response to laser light in C^+ , complete with a detailed comparison of the dynamics arising from different initial magnetic orientations ($M = 0$ or $M = 1$) [16, 17]. More recently the method has been extended to address HG [18], uncovering multielectron interference leading to resonant enhancement of HG from argon [19] and multichannel interference leading to suppression of HG in Ar^+ [20]. It is this Ar^+ system which occupies us in this article: accurate treatment of the electron emission channels associated with the different, closely-spaced

$3s^23p^4$ thresholds requires a method capable of describing both multielectron and multichannel effects.

The results contained in this article extend the work presented in [20] to investigate the effect of the initial magnetic quantum number, M , on HG. Although ground-state noble gas targets, predominantly used in HG experiments, can only have $M = 0$, it has been suggested that the highest harmonics produced from Ar arise from ionized species generated during the laser-Ar interaction [21–23]. We have previously demonstrated [20] that despite the general assumption that a higher ionization potential leads to a lower harmonic yield [24], the yield from Ar^+ with $M = 0$ actually exceeds that of He, even though Ar^+ is more strongly bound. By analyzing the yield from $M = 1$ we can improve our understanding of how atomic structure affects HG.

The magnetic quantum number, M determines which radiative transitions are permitted according to the dipole selection rules. The first difference for $M \neq 0$ is that $\Delta L = 0$ transitions are allowed. We can thus have transitions from $^2P^o$ states to $^2P^e$ and $^2D^e$ states. Further changes arise as for $M = 0$ the five $3p$ electrons occupy $m = \{-1, -1, 0, 1, 1\}$, whereas for $M = 1$ they occupy $m = \{-1, 0, 0, 1, 1\}$. Thus, $M = 1$ has two $m = 0$ electrons in the outer shell while $M = 0$ has only one; it is these $m = 0$ electrons which dominate the response to the laser field. Furthermore, for $M = 1$, emission of an $m = 0$ electron leaves $3p^4$ in $\{-1, 0, 1, 1\}$, which can form both triplet and singlet spin. Conversely, for $M = 0$, emission of an $m = 0$ electron leaves $3p^4$ in $\{-1, -1, 1, 1\}$, which couples only to singlet spin. Hence emission of an $m = 0$ electron leaving Ar^{2+} in its $^3P^e$ ground state is possible only for $M = 1$. This change may lead to enhanced ionization: application of the ADK formula [25] suggests that the ionization rate could be increased by a factor of 5 in the $M = 1$ case. Finally, for $M = 0$, ionization can proceed via intermediate excitation of the $3s3p^6 \ ^2S$ bound-state. However, specifying $M = 1$ precludes the system having S symmetry. It is therefore of interest to study how a change in M affects HG for Ar^+ .

II. THEORY

A full account of the TDRM method for $M \neq 0$ can be found in [15, 17], and the extension of TDRM to HG in [18]. Here we give only a brief overview. TDRM employs the standard R-matrix partition of space such that within a particular radius of the nucleus all interactions between electrons are fully described. Should a photoionized electron pass beyond the boundary of this region it becomes spatially isolated from the residual ion. Electron-exchange effects can then be neglected, and the electron moves only in the long-range potential of the residual ion and the laser field. Then, starting from a field-free solution, the time-dependent Schrödinger equation can be solved, using a Crank-Nicolson scheme to propagate the wavefunction in time.

HG arises from the laser-driven oscillation of the atomic dipole. The harmonic spectrum is proportional to the charge's acceleration, but can be calculated via either the dipole length or velocity. In TDRM theory, both methods give the same result to a high level of accuracy for He [18]. The spectra shown here are calculated from the expectation value of the dipole length operator:

$$\mathbf{d}(t) \propto \langle \Psi(t) | \mathbf{z} | \Psi(t) \rangle, \quad (1)$$

where \mathbf{z} is the total position operator along the laser polarization axis. The harmonic spectrum is then proportional to

$$\omega^4 |\mathbf{d}(\omega)|^2, \quad (2)$$

where ω is the laser frequency and $\mathbf{d}(\omega)$ is the Fourier transform of $\mathbf{d}(t)$. With this approach we can extract the single-atom/ion response of the system. We do not consider macroscopic effects, but rather treat the single-atom in a level of detail not afforded by any other method.

III. COMPUTATIONAL SETUP

The Ar^+ targets used in this article are as described in [20]. We calculate the $3s^23p^4$ and $3s3p^5$ eigenstates of Ar^{2+} via configuration-interaction calculations, and describe Ar^+ as one of these states plus an additional electron. This method allows us to vary systematically the atomic structure contained in the calculations, and assess the effects of including various thresholds. We employ several models in our calculations. The five-state description comprises all five Ar^{2+} thresholds. The three-state model includes only the $3s^23p^4$ thresholds. We also use models which comprise individual $3s^23p^4$ $^3P^e$, $^1D^e$ or $^1S^e$ thresholds with or without the $3s3p^5$ thresholds. The initial state is the Ar^+ $3s^23p^5$ ground-state with $M = 1$.

As described above, exchange effects are included within a radius of 15 a.u. of the nucleus. We use 60 B-splines per angular momentum for the description of the continuum orbitals. The Ar^+ basis then comprises all allowed combinations of these continuum orbitals with

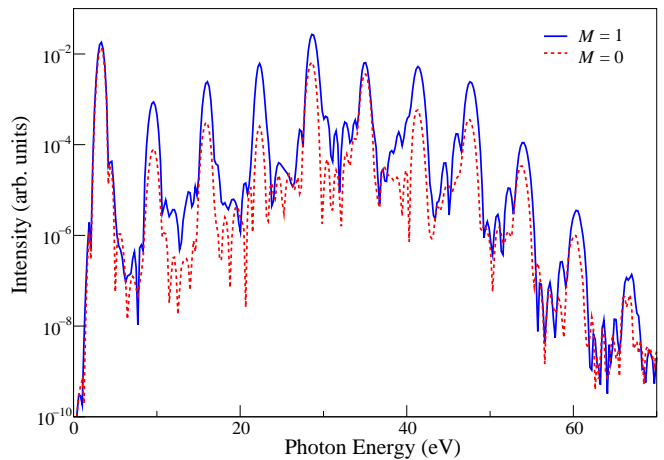


FIG. 1: (Color online) The harmonic spectra produced by Ar^+ in the three-state model (see text) for a 390-nm, $4 \times 10^{14} \text{ Wcm}^{-2}$ laser pulse, from both the $M = 0$ (red dashed line) and $M = 1$ (blue, solid line) initial alignment. $M = 0$ results previously published in [20].

the Ar^{2+} states up to a maximum angular momentum of $L = 19$. The outer region is divided into sectors of 2 a.u. each containing 35 9th order B-splines. The time-step for the wavefunction propagation is 0.1 a.u. We use a 390-nm, $4 \times 10^{14} \text{ Wcm}^{-2}$ spatially homogeneous and linearly polarized laser pulse comprising a 3-cycle \sin^2 ramp-on/ramp-off, and 2 cycles at peak intensity.

IV. RESULTS

Figure 1 shows the harmonic spectrum produced by the three-state Ar^+ target in both the $M = 1$ and $M = 0$ initial alignments. The ionization yield from $M = 1$ is four times larger than that from $M = 0$, and we might naively assume that the $M = 1$ harmonic yield should increase correspondingly. While an increase is evident, the enhancement of the $M = 1$ harmonic yield is not trivially proportional to the increase in the level of ionization. In general, the $M = 0$ harmonic peak values are between 10% and 30% of the equivalent $M = 1$ peaks, except in the 1st, 7th and 11th harmonics, where the $M = 0$ peaks are 77%, 4% and 55% of the $M = 1$ values respectively. On average the $M = 1$ yield is four times larger than for $M = 0$, which is in line with the increase in ionization.

To assess the physics underlying the changes between the $M = 0$ and $M = 1$ harmonic spectra, we analyze the changes effected by the description of the atomic structure. These changes are shown most dramatically by considering the harmonic response of Ar^+ when only a single state of the $3s^23p^4$ configuration is included. Figure 2 compares the spectra for $M = 1$ and $M = 0$ calculations in which the individual $3s^23p^4$ $^3P^e$ and $^1D^e$ thresholds, and both $3s3p^5$ thresholds are included. The yield obtained in the $^3P^e$ threshold calculation is dramatically enhanced for $M = 1$: the harmonic peaks below the ion-

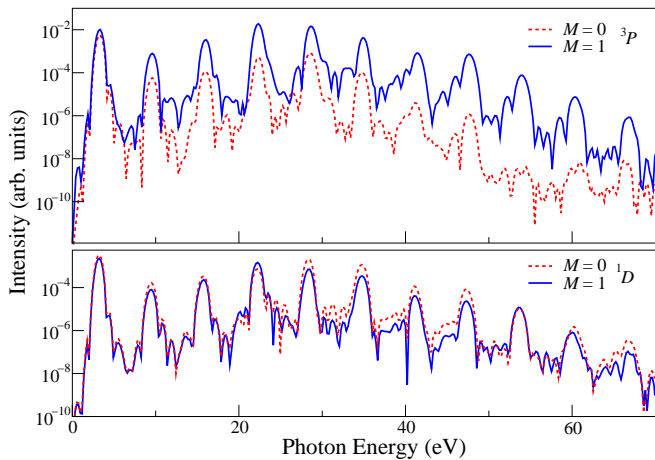


FIG. 2: (Color online) The harmonic spectra produced from the individual 3P (upper) and 1D (lower) threshold description of Ar^+ with both $3s3p^5$ thresholds also active, for $M=0$ (red, dashes) and $M=1$ (blue line). $M=0$ results from [20].

ization energy are increased by a factor of 30, while those above are increased by several orders of magnitude. This is mainly due to a 10-fold increase in the ionization yield associated with the $^3P^e$ threshold for $M=1$. The increased harmonic yield associated with the $^3P^e$ threshold does not substantially affect the $^1D^e$ spectrum, which is reduced by only 30% on average. Ionization towards the 1D threshold also shows a 30% decrease from $M=0$ to $M=1$, which agrees with naive statistical calculations of the ionization probabilities.

For $M=0$ it was found that the dominant contribution to the harmonic yield was from channels connected to the first excited threshold- $3s^23p^4$ $^1D^e$. However, for $M=1$ harmonic radiation stems primarily from the Ar^{2+} ground-state threshold- $3s^23p^4$ $^3P^e$. For $M=1$, $m=0$ electron emission channels associated with the $^3P^e$ state of Ar^{2+} are available, but they are not for $M=0$. A secondary factor is the presence of two $m=0$ electrons for $M=1$ compared to only one for $M=0$. Consequently, Fig. 2 shows a dramatic increase in the efficiency of HG for $M=1$ compared to $M=0$ in the $^3P^e$ calculation.

Figure 2 shows the dramatic effect of the presence of $m=0$ emission channels on the physics of HG. The $^3P^e$, $M=0$, spectrum shows a strong harmonic response up to the ionization threshold at 27 eV, but then falls off abruptly above this energy. The $M=1$ spectrum shows the more characteristic plateau of harmonics, extending to 45 eV, approximately equal to the expected cut-off energy [26]. Thus the $M=1$ spectrum shows features consistent with the predictions of the recollision model, whereas the $M=0$ spectrum does not. Hence, a small change in the magnetic quantum number can affect dynamics in a fundamental manner. In this case, the interaction between the initial state and the continuum associated with the $^3P^e$ threshold, critical for HG, has been altered on a fundamental level.

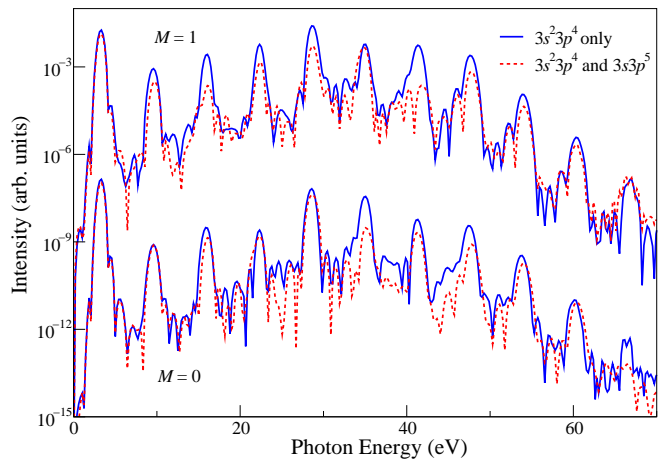


FIG. 3: (Color online) The harmonic spectra produced by the three- and five-state models of Ar^+ for $M=0$ and $M=1$. The $M=0$ spectra have been offset by a factor of 10^5 , and were previously published in [20].

Figure 2 shows a slight increase in the $^1D^e$ yield for $M=0$ which may be due to the coupling of the $3s3p^6$ 2S and $3s^23p^4nd$ 2S states. For $M=1$, the 2S states cannot be excited and hence the $3s3p^6$ state cannot act as an intermediate resonance. From the separate $^1D^e$ and $^3P^e$ spectra, Fig. 2 implies that the HG mechanism has changed completely with an apparently small change in the atomic structure of the target, and suggests that the three-step model may require extensions for the description of HG in general systems.

The total harmonic yield cannot be approximated by that of a single threshold, nor by trivially summing the individual contributions. Adding the $^3P^e$ and $^1D^e$ spectra overestimates the total yield by as much as a factor of 20 for the 5th and 7th harmonics. Interferences between the $^3P^e$ and $^1D^e$ channels lead to suppression of the harmonic yield. The yield from the 1S threshold is four orders and two orders of magnitude smaller than that from the $^3P^e$ or $^1D^e$ thresholds respectively. Multichannel effects involving the 1S threshold do not have as dramatic an influence as $^3P^e$, $^1D^e$ interferences, but still lead to a 50% reduction in several harmonic peaks.

In addition to these multichannel effects, the system also exhibits interference between the response of $3s$ and $3p$ electrons. Figure 3 shows the effect of including the $3s3p^5$ thresholds on the overall harmonic yield for both $M=0$ and $M=1$. There are noticeable differences in the way these interferences affect HG for the different values of M . Including the $3s3p^5$ thresholds in the $M=1$ calculation leads to a factor 24 reduction in the 13th harmonic peak, the energy of which coincides with the $3s3p^5$ $^3P^o$ threshold. There is an order of magnitude reduction at the 5th harmonic and the 3rd, 7th, 9th and 15th peaks are all reduced by between three and five times. In the $M=0$ spectrum the largest effect of this inclusion is an order of magnitude decrease in the 11th harmonic peak, with significant reductions also observed

at the 13th and 15th, and a 50% suppression of the 5th harmonic.

The main difference between the spectra is thus that the harmonics below the ionization threshold (3rd-9th) are more significantly reduced for $M = 1$ than for $M = 0$. This can be understood in terms of field-driven, single-electron transitions between $3s^23p^4nl$ and $3s3p^5nl$ Rydberg states. Because of the increased importance of the $^3P^e$ threshold in the $M = 1$ calculation a significant population in $^3P^e nl$ Rydberg states is expected. These couple to the $^3P^o nl$ states via excitation of a $3s$ electron to $3p$. Such transfer may affect the coherent phase of the $3p$ electrons, thus suppressing harmonic radiation which depends strongly on this coherence. While such transitions are also expected for $M = 0$, the low yield from the $^3P^e$ threshold reduces the appearance of the effect. Single-electron transitions between the $3s^23p^4(^1D^e)nl$ or $(^1S^e)nl$ and $3s3p^5(^1P^o)nl$ states are also important but the larger energy gap – 7 photons in our calculations versus 5 photons for the $^3P^e \rightarrow ^3P^o$ transitions – may reduce the impact on the low-energy harmonics for $M = 0$. We note, however, that the effect may be stronger in practice: using experimental energies the energy gap corresponds approximately to a four-photon transition in both cases.

Inclusion of the $3s3p^5$ thresholds has a noticeable effect on the 11th to 15th harmonics, as shown in Fig. 3. For $M = 1$, we see a reduction in the intensity of the 13th harmonic by 1.5 orders of magnitude. This photon energy overlaps the Rydberg series leading up to the $3s3p^5\ ^3P^o$ threshold. With the dominant channels for HG being those connected with $^3P^e$, $3s - 3p$ transitions connect the important $3s^23p^4\ (^3P^e)\ nl$ states with $3s3p^5\ (^3P^o)\ nl$ states. This coupling could strongly influence the 13th harmonic. Similarly, for $M = 0$, the dominant $^1D^e$ threshold can couple to the $^1P^o$ threshold, leading to suppression of HG in the $3s3p^5\ (^1P^o)\ nl$ energy range – the 15th harmonic in our calculation. This interference is also responsible for the decrease in the 11th harmonic for $M = 0$, but the dominance of the $^3P^e$ channel means that this interference has little effect for $M = 1$.

V. DISCUSSION

The noticeable increase in the harmonic yield for $M = 1$ relative to $M = 0$ is of significant importance for both theoretical and experimental treatment of HG. From a theoretical standpoint, it is clear that apparently small details of atomic structure can have a large bearing on the single-atom response to laser light. It will be of great interest to see how experiment will bear out these findings, as methods of extracting the single atom response from a macroscopic picture will need to be developed.

Experimentally, the highest harmonics from Ar have been attributed to HG from Ar^+ [21, 22]. This constitutes a sequential process wherein Ar first ionizes and then undergoes HG. Although ionization by a linearly polarized laser field will leave Ar^+ predominantly in the

$M = 0$ state, the ion will subsequently evolve via the spin-orbit interaction. After 12 fs a significant $M = 1$ population will arise. This transfer to $M = 1$ can then lead to a significant enhancement of the harmonic response of Ar^+ . It would be of interest to investigate experimentally whether there are fundamental differences in HG from Ar^+ or Ar for different pulse lengths.

Given the significant enhancement of the harmonic yield demonstrated here, and the drive to improve the conversion efficiency of HG [27], it is evident that the development of a theoretical method incorporating the spin-orbit effect is of pressing importance. Such a method will yield theoretical data invaluable in directing experiment, and permit a more detailed analysis of the complex dynamics of ultrafast processes. To our knowledge, no method currently exists which comprises the spin-orbit, multielectron and multichannel interactions, but work is ongoing to extend TDRM theory to this end.

VI. CONCLUSION

We have used the TDRM method to describe HG from Ar^+ in both the $M = 0$ and $M = 1$ initial alignments. The harmonic yield from $M = 1$ is enhanced by 4 times, on average, over the $M = 0$ yield, although there is a non-uniform increase across the spectrum. There is a noticeable difference in the way that atomic structure affects the harmonic yield between $M = 0$ and $M = 1$. The dominant channels for HG are those connected to the ground ($^3P^e$) state of the Ar^{2+} ion, which is at variance with the $M = 0$ case where the first excited ($^1D^e$) state dominates. We have shown that multielectron and multichannel interferences are observed for $M = 1$, despite the apparent dominance of the $^3P^e$ threshold. In the $M = 1$ case these interferences lead to a more pronounced suppression of the harmonic yield than for $M = 0$.

While these calculations have been carried out using a wavelength of 390-nm we expect that the conclusions are applicable for longer wavelengths. The energy gap between the three lowest ionization thresholds in Ar^+ is approximately equal to that of an 800-nm photon, and even if the channels associated with higher lying thresholds were disfavoured at longer wavelengths, we have shown that even channels with a very small contribution to the total ionization yield can have a large impact on the total harmonic spectrum. The significant influence of multielectron and multichannel effects on the process demonstrates that a multielectron code, such as TDRM theory, or R-matrix incorporating time (RMT) [28], is essential for the accurate description of HG.

VII. ACKNOWLEDGEMENTS

ACB acknowledges support from DEL (NI). HWH is supported by EPSRC under grant number G/055416/1.

-
- [1] P. B. Corkum, *Phys. Today* **64**, 36 (2011).
- [2] K. Zhao, Q. Zhang, M. Chini, Y. Wu, X. Wang, and Z. Chang, *Opt. Lett.* **37**, 3891 (2012).
- [3] T. Popmintchev *et al.*, *Science* **336**, 1287 (2012).
- [4] M. Uiberacker *et al.*, *Nature* **446**, 627 (2007).
- [5] E. Goulielmakis *et al.*, *Nature* **466**, 739 (2010).
- [6] H. J. Wörner, J. B. Bertrand, D. V. Karashov, P. B. Corkum, and D. M. Villeneuve, *Nature* **466**, 604 (2010).
- [7] B. K. McFarland, J. P. Farrell, P. H. Bucksbaum, and M. Gühr, *Science* **322**, 1232 (2008).
- [8] O. Smirnova, Y. Mairesse, S. Patchkovskii, N. Dudovich, D. Villeneuve, P. B. Corkum, and M. Y. Ivanov, *Nature* **460**, 972 (2009).
- [9] N. Rohringer and R. Santra, *Phys. Rev. A* **79**, 053402 (2009).
- [10] A. D. Shiner, B. E. Schmidt, C. Trallero-Herrero, H. J. Wörner, S. Patchkovskii, P. B. Corkum, J.-C. Kieffer, F. Légaré, and D. Villeneuve, *Nat. Phys.* **7**, 464 (2011).
- [11] P. B. Corkum, *Phys. Rev. Lett.* **71**, 1994 (1993).
- [12] M. Lewenstein, P. Balcou, M. Y. Ivanov, A. L’Huillier, and P. B. Corkum, *Phys. Rev. A* **49**, 2117 (1994).
- [13] K. C. Kulander, K. J. Schafer, and J. L. Krause, *Int. J. Quantum Chem.* **40**, 415 (1991).
- [14] I. A. Ivanov and A. S. Kheifets, *Phys. Rev. A* **79**, 053827 (2009).
- [15] M. A. Lysaght, H. W. van der Hart, and P. G. Burke, *Phys. Rev. A* **79**, 053411 (2009).
- [16] M. A. Lysaght, P. G. Burke, and H. W. van der Hart, *Phys. Rev. Lett.* **102**, 193001 (2009).
- [17] S. Hutchinson, M. A. Lysaght, and H. W. van der Hart, *J. Phys. B: At. Mol. Opt. Phys.* **44**, 215602 (2011).
- [18] A. C. Brown, D. J. Robinson, and H. W. van der Hart, *Phys. Rev. A* **86**, 053420 (2012).
- [19] A. C. Brown, S. Hutchinson, M. A. Lysaght, and H. W. van der Hart, *Phys. Rev. Lett.* **108**, 063006 (2012).
- [20] A. C. Brown and H. W. van der Hart, *Phys. Rev. A* **86**, 063416 (2012).
- [21] M. Zepf, B. Dromey, M. Landreman, P. Foster, and S. M. Hooker, *Phys. Rev. Lett.* **99**, 143901 (2007).
- [22] E. A. Gibson, A. Paul, N. Wagner, R. Tobey, S. Backus, I. P. Christov, M. M. Murnane, and H. C. Kapteyn, *Phys. Rev. Lett.* **92**, 033001 (2004).
- [23] C.-G. Wahlström, J. Larsson, A. Persson, T. Starczewski, S. Svanberg, P. Salières, P. Balcou, and A. L’Huillier, *Phys. Rev. A* **48**, 4709 (1993).
- [24] X. F. Li, A. L’Huillier, M. Ferray, L. A. Lompré, and G. Mainfray, *Phys. Rev. A* **39**, 5751 (1989).
- [25] M. V. Ammosov, N. B. Delone, and V. P. Krainov, *Zh. Eksp. Teor. Fiz.* **91**, 2008 (1986).
- [26] J. L. Krause, K. J. Schafer, and K. C. Kulander, *Phys. Rev. Lett.* **68**, 3535 (1992).
- [27] F. Brizuela, C. M. Heyl, P. Rudawski, D. Kroon, L. Radling, J. M. Dahlström, J. Mauritsson, P. Johnsson, C. L. Arnold, and A. L’Huillier, *Sci. Rep.* **3**, 1410 (2013).
- [28] L. R. Moore, M. A. Lysaght, L. A. A. Nikolopoulos, J. S. Parker, H. W. van der Hart, and K. T. Taylor, *J. Mod. Optics* **58**, 1132 (2011).